Science of Sintering, **44** (2012) 331-339

doi: 10.2298/SOS1203331L

UDK 519.224;621.355.8;577.353

Characterization of Nanostructured Spinel $NiFe_2O_4$ Obtained by Soft Mechanochemical Synthesis

Z. Ž. Lazarević[1,*], Č. Jovalekić[2], D. Sekulić[3], M. Slankamenac[3], M. Romčević[1], A. Milutinović[1], N. Ž. Romčević[1]

[1]Institute of Physics, University of Belgrade, Pregrevica 118, Zemun, Belgrade, Serbia
[2]The Institute for Multidisciplinary Research, University of Belgrade, Belgrade, Serbia
[3]Faculty of Technical Sciences, University of Novi Sad, Novi Sad, Serbia

Abstract:

Powdery nickel ferrite, $NiFe_2O_4$ has been obtained by soft mechanochemical synthesis in a planetary ball mill. $Ni(OH)_2$ and $Fe(OH)_3$ are used as initial compounds. This mixture was mechanically activated for 25h, uniaxial pressed and sintered at 1100 ℃ for 2h. The phase composition of the sintered sample was analyzed by X-ray diffraction (XRD), energy dispersive spectrometer (EDS) and Raman spectroscopy. Morphologies were examined by scanning electron microscopy (SEM). The electrical DC/resistivity/conductivity at different temperatures was measured using a Source Meter Keithley 2410. An Impedance/Gain-Phase Analyzer (HP-4194) was used to measure the impedance spectra (100Hz - 10MHz) at different temperatures.

Keywords: *$NiFe_2O_4$, Raman spectroscopy, DC conductivity, Complex impedance.*

1. Introduction

Cubic nanosized spinel ferrites with the general formula MFe_2O_4 are well-known, important materials for applications such as high-density information storage media, for drug delivery, medical diagnostics, ferrofluid technology, electronic devices, catalysts, sensor technology and microwave applications [1-5]. The interests for using of these material permanently increases because of their usability under extreme conditions. They possess unique magnetic, chemical and mechanical properties. It is well known that properties of ferrite materials strongly depend on the preparation conditions. One of the most interesting ferrites is nickel ferrite $NiFe_2O_4$.

Synthesis of $NiFe_2O_4$ is mainly based on chemical and solid-state reaction methods. The many types of preparation and processing techniques including, for example, hydrothermal reactions [6], coprecipitation [7], micelle technique [8], sol-gel method [9], solid-state reaction [10] and the nonconventional mechanochemical route [11] has been recognized as a powerful method for the production of novel, high-performance, and low-cost materials. Other possibility is solid-state reaction during mechanical activation initiating by intensive milling in high-energy ball mills. The conventional solid-state reaction normally requires high temperature. Formation of the produced phase proceeds at interfaces of the reactants and product barrier layer prevents further reaction without elevating temperature. Due to reducing particle sizes and increasing in the contents area of reactant particles, solid-

*) **Corresponding author:** lzorica@yahoo.com **or** lzorica@ipb.ac.rs

state reactions during milling can proceed without the diffusion through the product layer and occurs at lower temperature.

The mechanochemical synthesis can deliver the designed phases and structures by a single-step of the high-energy milling conducted in an enclosed activation chamber at room temperature [12]. Usually, the compete formation of spinel ferrites was obtained only after milling followed by sintering, i.e. by employing two processing steps. It is obvious that the combined mechanochemical-thermal treatment yields a well-ordered spinel phase in ferrites at lower annealing temperatures and shorter durations than those required in conventional ceramic methods [13]. Of course, in such case the morphology of crystallite, agglomerate and particle is changed significantly.

Mechanochemical method, and primarily soft mechanochemically procedure is very suitable for the activation or synthesis of inorganic precursors. This is reflected primarily in the simplicity of the procedure and equipment used [12, 14]. In many cases, when it comes to classical synthesis reaction sintering process, requires high temperatures, which can present an additional problem in industrial production. Mechanochemical derived precursors exhibit significantly higher reactivity and thus lower the calcination and sintering temperature.

In this article, we demonstrated the synthesis of nanocrystalline $NiFe_2O_4$ through soft mechanochemical treatment, via high-energy milling of binary oxide precursors, starting from a mixture of the $Ni(OH)_2$ and $Fe(OH)_3$ powders in a planetary ball mill. The soft mechanochemical reaction leading to formation of the $NiFe_2O_4$ spinel phase was followed by X-ray diffraction, Raman spectroscopy and energy dispersive spectrometer. Scanning electron microscopy was used to analysed microstructure of the sintered sample. The electrical DC/resistivity/conductivity at different temperatures was measured to confirm the electrical character of these samples.

2. Experimental

In present work $NiFe_2O_4$ was prepared from stoichiometric quantities of $Ni(OH)_2$ and $Fe(OH)_3$ obtained via mechanochemical synthesis. $Fe(OH)_3$ has been synthesized from NaOH solution (25% mass) and $FeCl_3$ solution (25% mass). Mechanochemical synthesis was performed in air atmosphere in a planetary ball mill (Fritsch Pulverisette 5) for 25 h. Milling conditions were: hardened-steel vial of 500 cm^3 volume, filled with 40 hardened steel balls with a diameter of 13.4 mm, ball-to-powder weight ration 20:1 and determined at basic disc rotation speed 320 min^{-1} and rotation speed of discs with jars ~400 rpm. The powder mixture pressed into pallets using a cold isostatic press (8 mm in diameter and ~3 mm thick). Their powder mixture was sintered at 1100◦C for 2h (Lenton-UK oven) without pre-calcinations step. Heating rate was 10 °C min^{-1}, with nature cooling in air atmosphere. The formation of phase and crystal structure of $NiFe_2O_4$ were approved using the X-ray diffractometer (XRD, Model Philips PW 1050 diffractometer equipped with a PW 1730 generator, 40 kV x 20 mA, using Ni filtered CoK_α radiation of 1.78897 Å at the room temperature. Measurements were done in 2θ range of 10-80° with scanning step width of 0.05° and 10 s scanning time per step.

Raman measurements of sintered samples were performed using Jobin-Ivon T64000 monochromator. An optical microscope with 100x objective was used to focus the 514 nm radiation from a Coherent Innova 99 Ar^+ laser on the sample. The same microscope was used to collect the backscattered radiation. The dispersed scattering light was detected by a charge-coupled device (CCD) detection system. Room temperature Raman spectra are in spectral range from 100 to 800 cm^{-1}.

The morphology and microstructure of sintered samples were examined using scanning electron microscope (SEM, Model JEOL JSM-6460LV). The sintered samples in the disc shape were prepared for microstructure examination and electrical properties by polishing to thickness of 1 mm with silicon carbide and alumina powder and cleaning in an

ultrasonic bath in ethanol. The electrical DC/resistivity/conductivity in the temperature range 298-473 K was measured on a SourceMeter Keithley 2410. Impedance measurements were carried out in the frequency range 100 Hz to 10 MHz on a HP-4194A impedance/gain-phase analyzer using a HP-16048C test fixture in the temperature range 298-448 K. A personal computer with in-house-built software was used for acquisition of measured data.

3. Results and discussions

Formation mechanisms of materials from nanopowders by soft mechanically assisted synthesis (mechanochemical synthesis) are complex have not been fully understood yet. During the ferroelectric materials formation, the process passes through few steps. Generally, it starts with the decrease in particle and grain size of starting materials following by the nucleation and crystallization of target compound. As the result of mechanically assisted synthesis, nanocrystalline powders can be obtained directly from their hydoxide mixtures after milling.

The Fig. 1 shows the X-ray diffraction spectra of $NiFe_2O_4$ after sintering at 1100 ºC for 2h. All peaks detected at the 2θ = 22.21º, 36.13º, 42.50º, 44.35º, 51.63º, 64.12º, 68.53º and 75.51º clearly pointed to the formation of the new phase of $NiFe_2O_4$ (JCPDS card 89-7412). The peaks are well indexed to the crystal plane of spinel ferrite (k h l) (111), (220), (311), (222), (400), (422), (511) and (440), respectively. This confirms that the mechanochemical synthesis of $NiFe_2O_4$ is feasible and complete after 25 h milling time of the mixture of the hydroxides and sintered at 1100 °C for 2 h. The mean size, L = 56.3 nm, of crystallites is calculated by Scherrers equation:

$$L = \lambda_{Co} / [w(2\theta) \cdot \cos\theta]$$

where w(2θ) is peak width in radians, 2θ is peak position and λ_{Co} = 1.78897 Å wavelength of used X-ray source.

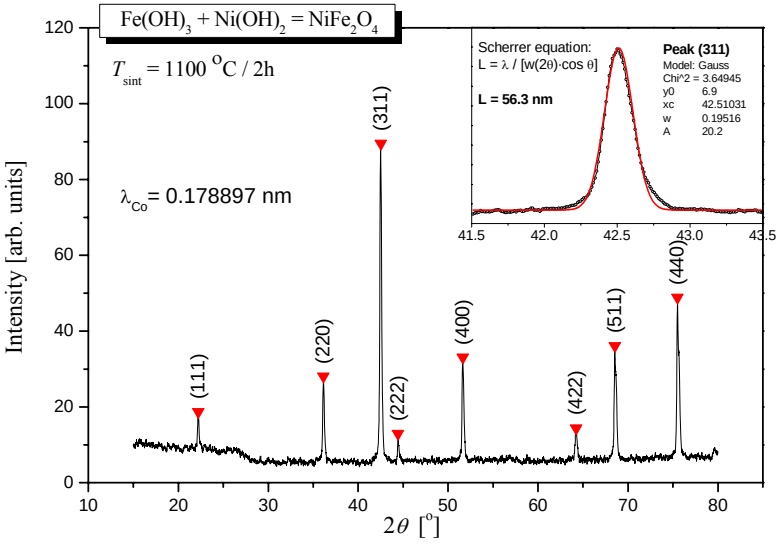

Fig. 1. X-ray diffraction pattern of the $NiFe_2O_4$ sintered at 1100 °C for 2 h.

The Fig. 2 shows Raman spectra for the $NiFe_2O_4$ prepared by the soft mechanochemical synthesis. To simplify, peaks are assigned as for normal spinel structure. But, all five Raman peaks are asymmetric (or dissociated). Each peak can be presented like a doublet, what is a characteristic of the inverse spinel structure. At a microscopic level the

structure of $NiFe_2O_4$ can be considered as a mixture of two sublattices with Fe^{3+} and Ni^{2+}. It is supposed that Fe^{3+} and Ni^{2+} are ordered over the A and B-sites.

The A_{1g} mode is due to symmetric stretching of oxygen atoms along Fe-O (and Ni-O) bonds in the tetrahedral coordination. E_g is due to symmetric bending of oxygen with respect to the metal ion and $F_{2g}(3)$ is caused by asymmetric bending of oxygen. $F_{2g}(2)$ is due to asymmetric stretching of Fe (Ni) and O. $F_{2g}(2)$ and $F_{2g}(3)$ correspond to the vibrations of octahedral group. $F_{2g}(1)$ is due to translational movement of the tetrahedron (metal ion at tetrahedral site together with four oxygen atoms). There is a negligible displacement of metal atoms in modes A_{1g}, E_g and $F_{2g}(3)$ [15].

All five Raman peaks are asymmetric, with shoulder on the low energy side. Each peak can be presented like a doublet. At a microscopic level the structure of $NiFe_2O_4$ can be considered as a mixture of two sublattices with Fe^{3+} and Ni^{2+}. It is supposed that Fe^{3+} and Ni^{2+} are ordered over the B-sites. In nanocrystalline samples asymmetry is partly due to confinement and size-distribution of nanoparticles.

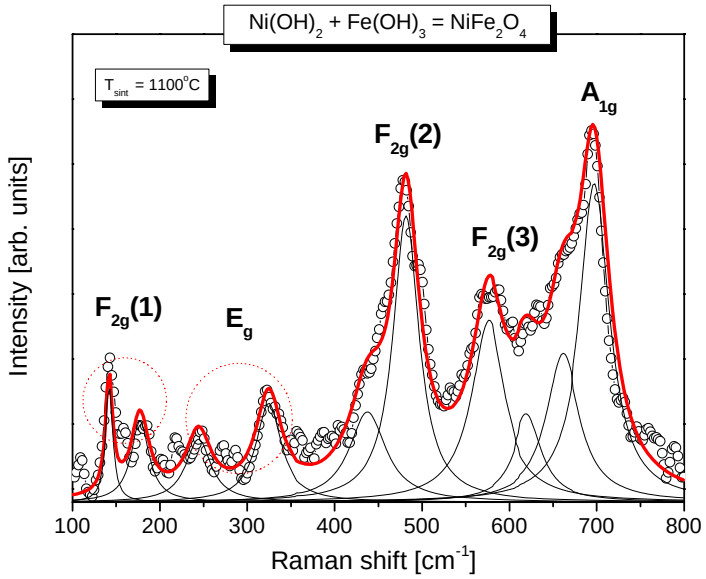

Fig. 2. Raman spectra for the sample of the $NiFe_2O_4$ sintered at 1100 °C for 2h.

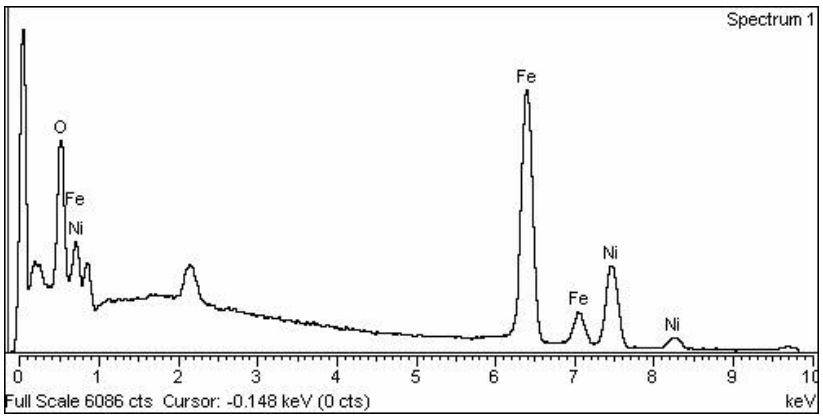

Fig. 3. EDS analysis of the $NiFe_2O_4$.

The composition of the product was analyzed by EDS measurements of several individual particles, as well as larger crystal clusters. The analyses show a constant Ni:Fe

atomic ratio of 1:2, which corresponds to the $NiFe_2O_4$ phase. Fig. 3 shows a typical EDS spectrum, recorded on the $Ni(OH)_2$ and $Fe(OH)_3$ sample milled for 25 h and sintered at 1100 °C for 2 h.

The Fig. 4 shows the microstructure of the $NiFe_2O_4$ ferrite. It can be observed that in sintered sample of ferrite exist polygonal grains. Having in mind that microstructure has strong influence on properties, detailed investigation on the sintering process and microstructure of the $NiFe_2O_4$ are in progress.

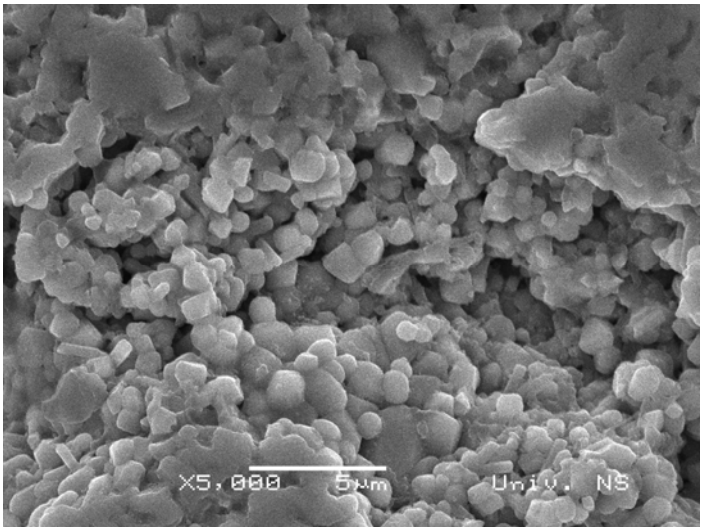

Fig. 4. SEM micrograph pattern of the $NiFe_2O_4$ sintered at 1100 °C for 2h.

Fig. 5 shows the variation of DC conductivity with temperature for the sample of $NiFe_2O_4$. The plot of $\log(\sigma_{DC})$ versus (1/T) shows that this dependence is linear for both sintered samples in a certain temperature range. Linear increase in the conductivity of sintered samples with temperature shows their semiconducting nature. The conductivity of ferrites is known to depend upon the purity of starting materials, sintering temperature and sintering time, which influence the microstructure and composition of the samples [16].

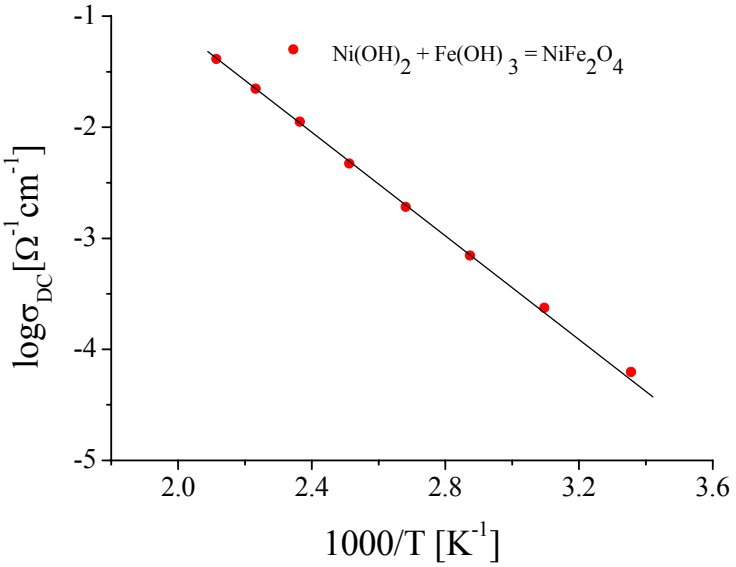

Fig. 5. Temperature dependence of DC electrical conductivity of ferrite samples.

The increase in DC conductivity with temperature is due to the increase in the thermally activated drift mobility of charge carriers according to the hopping conduction mechanism. The activation energy for the thermally activated hopping process was obtained by fitting the DC conductivity data with the Arrhenius relation [17]

$$\sigma_{DC}(T) = \sigma_0 \exp\left(-\frac{\Delta E}{kT}\right)$$

where σ_0 is the pre-exponential factor with the dimensions of $(\Omega cm)^{-1}K$, ΔE is the activation energy for DC conductivity, T is the absolute temperature and k is the Boltzmann's constant. The slope of the $\log(\sigma_{DC})$ versus (1/T) straight line is a measure of activation energy of the $NiFe_2O_4$ ferrite. The determined values for the conduction activation energy, ΔE is 0.452 eV (Fig. 5). There is no remarkable change in the slope of the measured temperature range, which indicates the fully inverse spinel structures of $NiFe_2O_4$.

The complex impedance spectroscopy [18] has been used to understand the electrical conduction mechanism of the synthesized ferrite. It helps in the separation of grain and grain boundary because each of them has different relaxation times, resulting in separate semicircles in complex impedance plot. Impedance data can be fitted and analyzed based on an idealized circuit model with discrete electrical components [19]. If the simple equivalent circuit (series array of parallel RC elements) is applied where each component (grain and grain boundary) is represented as a parallel RC element then the total complex impedance is [20, 21]:

$$Z^*(\omega) = \left(\frac{1}{R_g} + j\omega C_g\right)^{-1} + \left(\frac{1}{R_{gb}} + j\omega C_{gb}\right)^{-1}$$

where R_g and R_{gb} represent the grain and grain boundary resistance and C_g and C_{gb} represent the grain and grain boundary capacitance. Depending on the electrical properties of the material, the first semicircle in low frequency region represents the resistance of the grain boundary. The second one obtained for high frequency domain corresponds to the resistance of grain or bulk properties. The resistances are calculated from the circular arc intercepts on ReZ axis, while the capacitances are derived from the height of the circular arcs. The maximum value corresponds to the relaxation frequency. Typical values obtained for capacitance are in the pF range for grains and nF range for grain boundaries [22].

If the semicircles are depressed, then the electrical response exhibits distributed impedance and a distributing factor (n) in the equivalent circuit should be taken into account. Thus a constant phase element, CPE, is introduced. The CPE element can be used to replace the capacitor in each RC circuit [21, 23]. This element is used to model the ac response of non-homogenous systems. The impedance of a CPE can be described as [20]:

$$Z_{CPE} = A^{-1}(j\omega)^{-n}$$

where ω is the angular frequency, A and n ($0 \le n \le 1$) are fitted parameters. When n = 1, then the CPE describes an ideal capacitor with C = A, while when n = 0 the CPE describes an ideal resistor with R = 1/A. CPE elements in the equivalent circuit model have been used to describe non ideal Debye-like behavior [21] and enable taking into account phenomena occurring in the interface regions, associated with inhomogeneity and diffusion processes [23].

The complex impedance spectrum (ReZ vs. ImZ called Cole-Cole plot) for sintered $NiFe_2O_4$ ferrite as a function of frequency at different temperatures (293-448 K) are shown in Fig. 6. If we analyze the impedance response plotted for Ni ferrite, it is noticeable that the impedance spectrum includes both grain and grain boundary effects. No other relaxation mechanism, such as the electrode effect, is identified for the analyzed frequency range. Also, it is seen that the radius of curvature is decreased with increasing temperature which suggests a mechanism of temperature-dependent on relaxation.

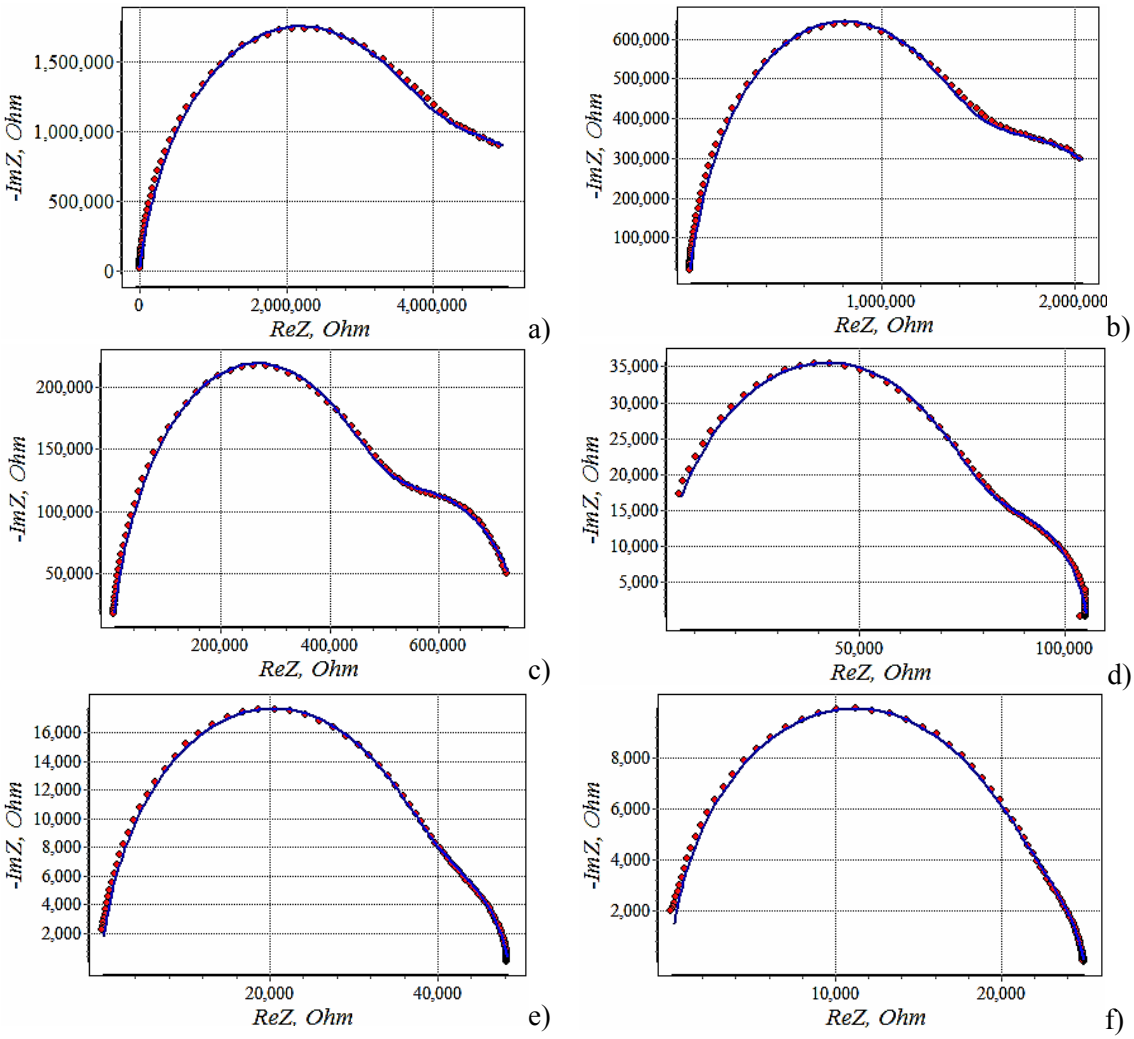

Fig. 6. Experimental (red points) and calculated (solid blue line) Cole-Cole plots for $NiFe_2O_4$ ferrite, sintered at 1100 °C and measured at: (a) 298 K, (b) 323 K, (c) 348 K, (d) 398 K, (e) 423 K, (f) 448 K.

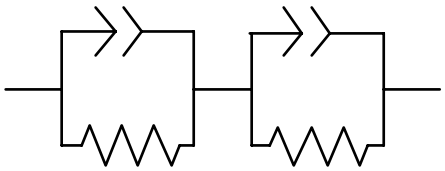

Fig. 7. Proposed equivalent circuit model for analysis of the impedance spectroscopy data.

Successful modeling of the impedance response (Cole-Cole plots) was achieved using an equivalent circuit consisting of two serially connected parallel R-CPE elements taking into account grain and grain boundary effects, see Figs. 6 and 7. Analysis and simulation of impedance spectra was performed using EIS Spectrum Analyzer software [24].

The different electrical parameters calculated from the complex impedance plots at selected temperatures are shown in Table I. The value of the grain boundary resistance is found to be larger than the resistance of the grain, $R_{gb} \geq R_g$. It is observed that the both resistances decrease with increasing temperature. It indicates that the conductivity increases with increase in temperature supporting the typical negative temperature coefficient of resistance (NTCR) behavior of $NiFe_2O_4$ usually shown by semiconductors. For all the temperatures the capacitance of the grain boundary is higher than that of the grain. The values for the distributing factor for grain and grain boundary contributions (n_g and n_{gb}) are in the range between 0.6 and 0.9 that is an indication of sample inhomogeneity due to the presence of two phases that was previously confirmed by EDS analysis.

Tab. I. Impedance parameters calculated from the complex impedance plots at different temperatures.

Temperature (K)	R_g (Ω)	C_g (F)	n_g	R_{gb} (Ω)	C_{gb} (F)	n_{gb}
298	2.397E6	4.487E-11	0.881	3.789E6	4.912E-9	0.688
323	1.051E6	4.590E-11	0.887	1.365E6	9.585E-9	0.649
348	2.915E5	4.525E-11	0.892	4.719E5	8.101E-9	0.713
398	2.572E4	3.949E-11	0.898	7.992E4	5.442E-9	0.822
423	1.043E4	3.104E-11	0.921	3.797E4	7.682E-9	0.789
448	4.281E3	2.605E-11	0.936	2.072E4	7.355E-9	0.794

4. Conclusions

$NiFe_2O_4$ ferrite powders have been prepared by soft mechanochemical synthesis starting from the mixture of the $Ni(OH)_2$ and $Fe(OH)_3$ powders. Single phase nanosized nickel-ferrite was synthesized by 25 h ball milling and sintered at 1100 °C for 2 h. X-ray diffraction of the prepared sample shows single phase cubic spinel structure. In the Raman spectra is bserved all of five first-order Raman active modes in the form characteristic for inverse spinel structure. The sintered sample of ferrite has polygonal grains. The analysis of the complex impedance data shows that the capacitive and reactive properties of the sintered $NiFe_2O_4$ ferrite are mainly attributed due to the processes which are associated with the grain and grain boundary. The grain and grain boundary resistances of sintered sample exhibit decreasing trends with the increase in temperature. It indicates that the conductivity increases with increase in temperature supporting the typical negative temperature coefficient of resistance (NTCR) behaviour of the material usually shown by semiconductors. Value of determined activation energy showed that conduction was due to electron hopping between Fe^{2+} and Fe^{3+}.

Acknowledgments

This research was financially supported by the Serbian Ministry of Education and Science through Projects No. III 45003 and III 45015.

References

1. R. H. Kodama, J. Magn. Magn. Mater. 200 (2000) 359-372.

2. H. Kavas, A. Baykal, M. S. Toprak, Y. Köseoğlu, M. Sertkol, B. Aktas, J. Alloys Compd. 479 (2009) 49-55.
3. J. A. C. de Paiva, M. P. F. Graça, J. Monteiro, M. A. Macedo, M. A. Valente, J. Alloys Compd. 485 (2009) 637-641.
4. A. Alarifi, N. M. Deraz, S. Shaban, J. Alloys Compd. 486 (2009) 501-506.
5. A. M. M. Farea, S. Kumara, K. M. Batoo, A. Y. C. G. Lee, Alimuddin, J. Alloys Compd. 469 (2009) 451-457.
6. J. Huo, M. Wei, Mater. Lett. 63 (2009) 1183-1184.
7. P. Sivakumur, R. Ramesh, A. Ramanand, S. Ponnusamy, C. Muthamizhchelvan, Mater. Lett. 65 (2011) 483-485.
8. A. Kale, S. Gubbala, R. D. K. Misra, J. Magn. Magn. Mater. 277 (2004) 350-358.
9. D. H. Chen, X. R. He, Mater. Res. Bull. 36 (2001) 1369-1377.
10. P. K. Roy, J. Bera, J. Mater. Process. Technol. 197 (2008) 279-283.
11. V. Šepelák, U. Steinike, D. C. Uecker, S. Wissmann, K. D. Becker, J. Solid State Chem. 135 (1998) 52-58.
12. E. Avvakumov, M. Senna, N. Kosova, Soft Mechanochemical Synthesis: A Basis for New Chemical Technologies, Kluwer Academic Publishers, Boston, 2001.
13. V. Šepelák, I. Bergmann, A. Feldhoff, P. Heitjans, F. Krumeich, D. Menzel, F. J. Litterst, S. J. Campbell, K. D. Becker, J. Phys. Chem. C 111 (2007) 5026-5033.
14. V. V. Boldyrev, Solid State Ionics 63-65 (1993) 537-543.
15. A. Ahlawat, V. G. Sathe, J. Raman Spectrosc. 42 (2011) 1087-1094.
16. P. A. Jadhav, R. S. Devan, Y. D. Kolekar, B. K. Chougule, J. Phy. Chem. Solids 70 (2009) 396-400.
17. S. M. Savic, M. V. Nikolic, O. S. Aleksic, M. P. Slankamenac, M. B. Zivanov, P. M. Nikolic, Sci. Sinter. 40 (2008) 27-32.
18. J. R. Macdonald, Impedance Spectroscopy, John Wiley and Sons, 1987.
19. Kumar, K. M. Batoo, R. Prakash, H. K. Choi, B. H. Koo, J. I. Song, H. Chung, H. Jeong, C. G. Lee, Journal of Central South University of Technology 17 (2010) 1133-1138.
20. R. Martinez, A. Kumar, R. Palai, J. F. Scott, R. S. Katiyar, J. Phys. D Appl. Phys. 44 (2011) 105302.
21. E. J. Abram, D. C. Sinclair, A. R. West, J. Electroceram. 10 (2003) 165-177.
22. A. R. West, D. C. Sinclair, N. Hirose, J. Electroceram. 1(1997) 65-71.
23. F. D. Morrison, D. J. Jung, J. F. Scott, J. Appl. Phys. 101 (2007) 094112.
24. A. S. Bondarenko and G. Ragoisha, EIS Spectrum Amalyzer, http://www.abc.chemistry.bsu.by

Садржај: *Прах никал ферита, $NiFe_2O_4$ је добијен млевемјем након 25h у планетарном млину са куглама софт механохемијском синтезом, пресовањем и синтеровањем на 1100°C за 2h. Фазни састав синтерованих узорака испитан је ренгено структурном анализом (XRD), енергетски-дисперзионом спектрометријом (EDS) и Раман спектроскопијом. Микроструктуре су испитане на скенирајућем електронском микроскопу (SEM). Електричне DC/отпорности/проводности на различитим температурама, измерене су помоћу Soyrce Meter Keithley 2410 уређаја. Импедансни спектри (100Hz-10MHz), на различитим температурама, измерене су помоћу Impedance/Gain-Phase Analyzer (HP-4194A) уређаја.*

Кључне речи*: $NiFe_2O_4$, Раман спектроскопија, DC проводност, комплексна импеданса.*